Supplement of The Cryosphere, 13, 237–245, 2019
https://doi.org/10.5194/tc-13-237-2019-supplement

The Cryosphere Open Access

Supplement of

Brief communication: Rapid machine-learning-based extraction and measurement of ice wedge polygons in high-resolution digital elevation models

Charles J. Abolt et al.

Correspondence to: Charles J. Abolt (chuck.abolt@utexas.edu)

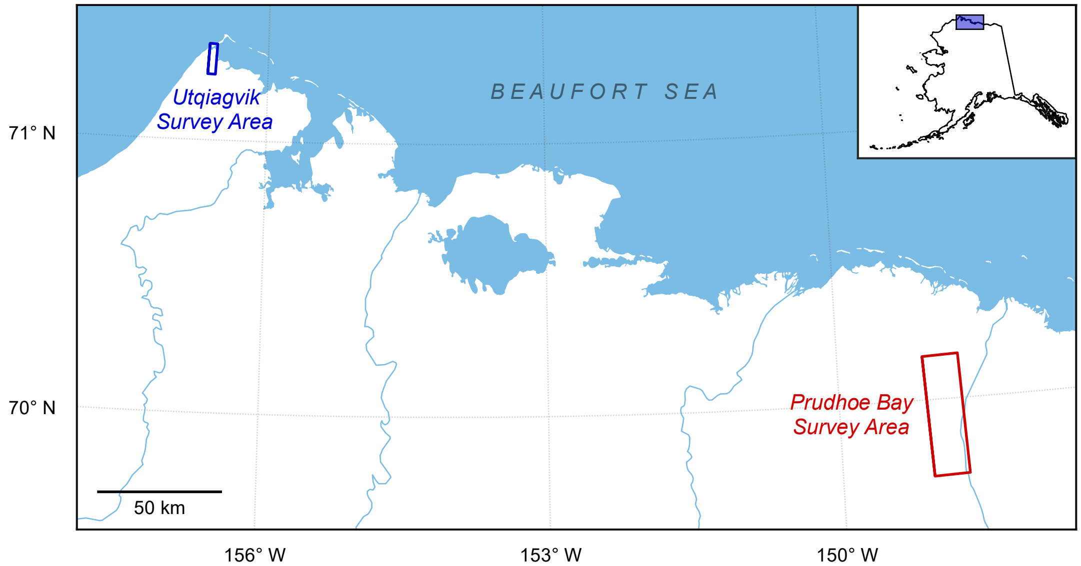

Figure S1. Bounding boxes of airborne lidar surveys.

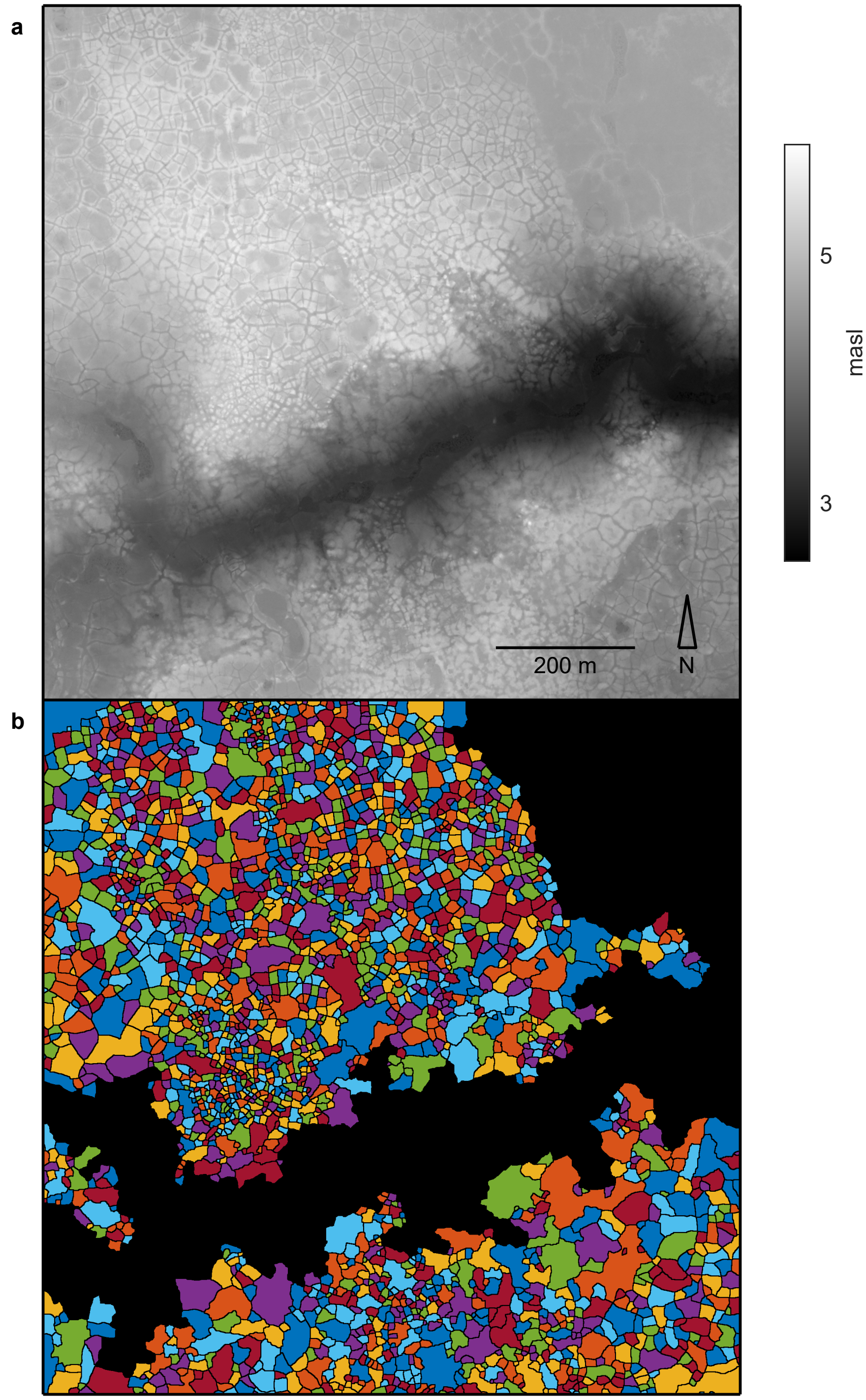

Figure S2. 50 cm DEM (**a**) and polygon delineation (**b**) at site Utqiagvik-1.

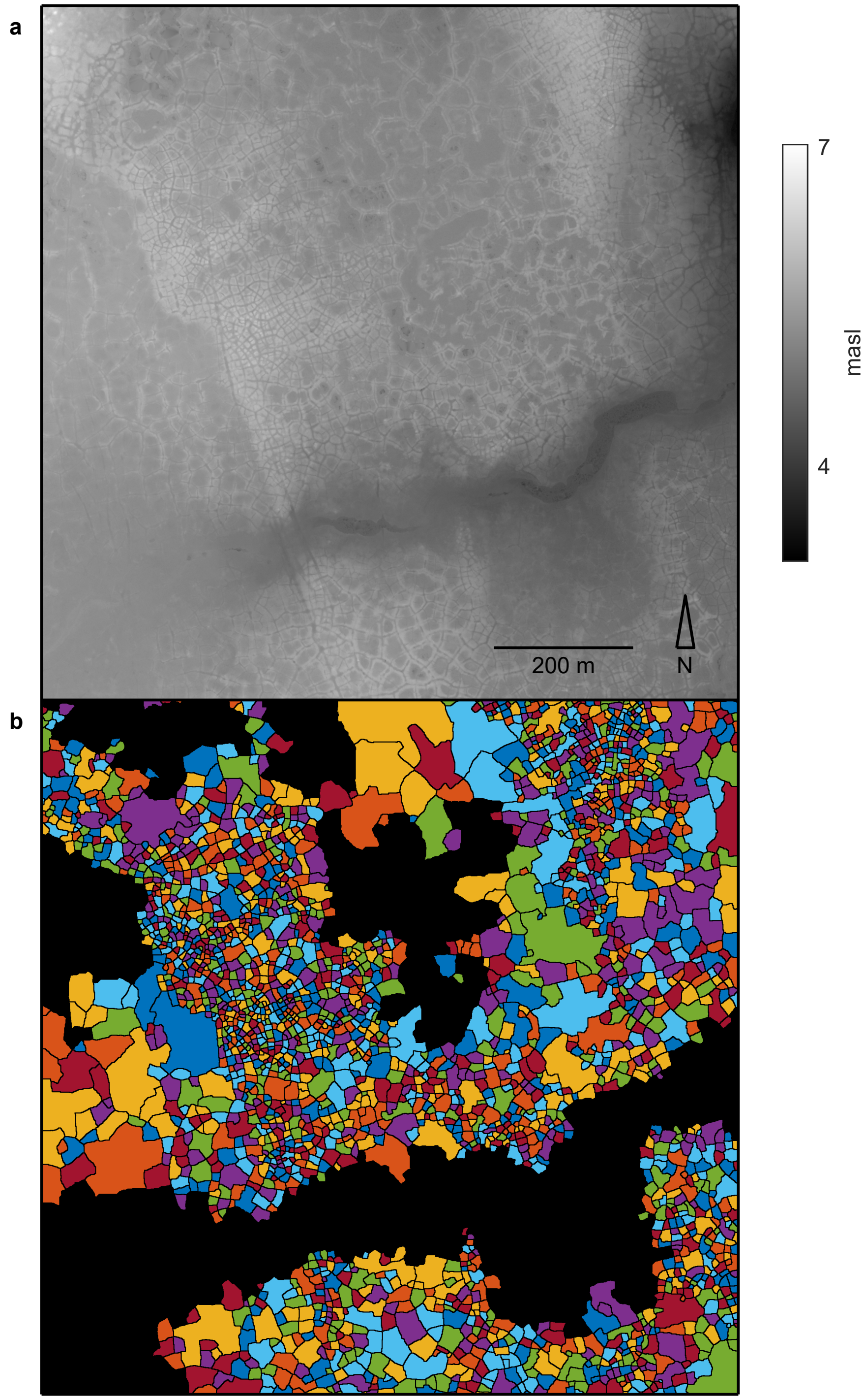

Figure S3. 50 cm DEM (**a**) and polygon delineation (**b**) at site Utqiagvik-2.

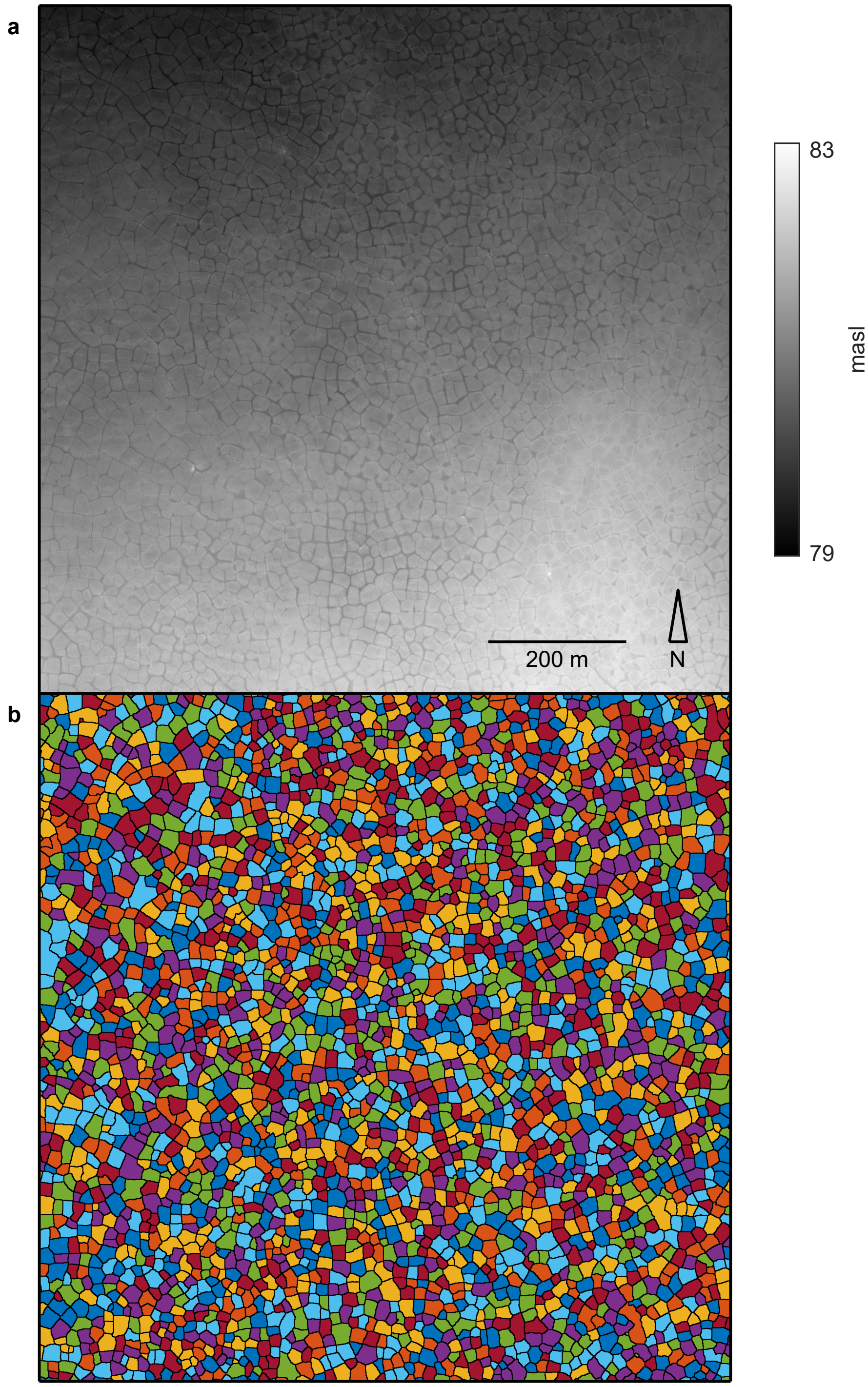

Figure S4. 50 cm DEM (**a**) and polygon delineation (**b**) at site Prudhoe-1.

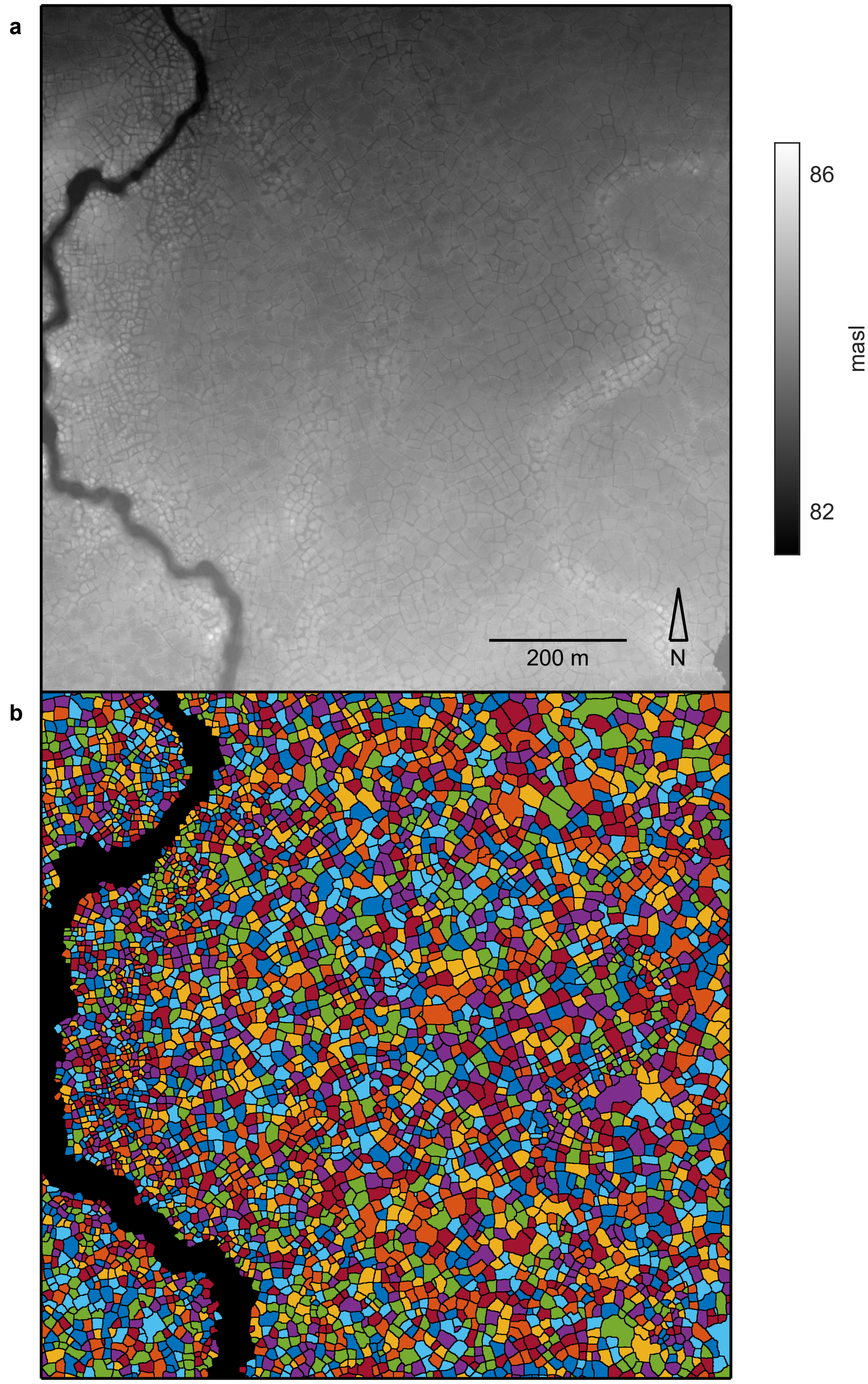

Figure S5. 50 cm DEM (**a**) and polygon delineation (**b**) at site Prudhoe-2.

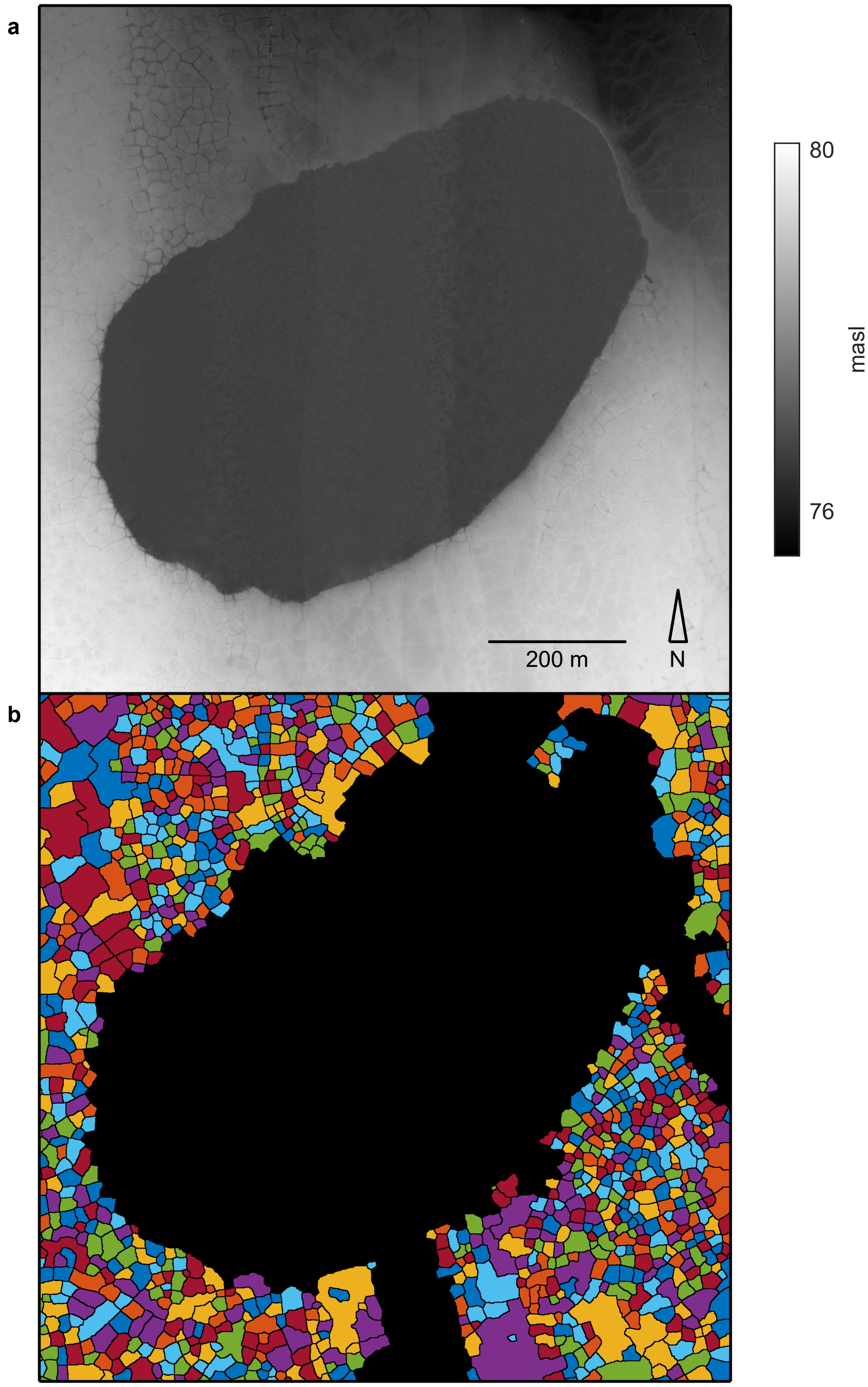

Figure S6. 50 cm DEM (**a**) and polygon delineation (**b**) at site Prudhoe-3.

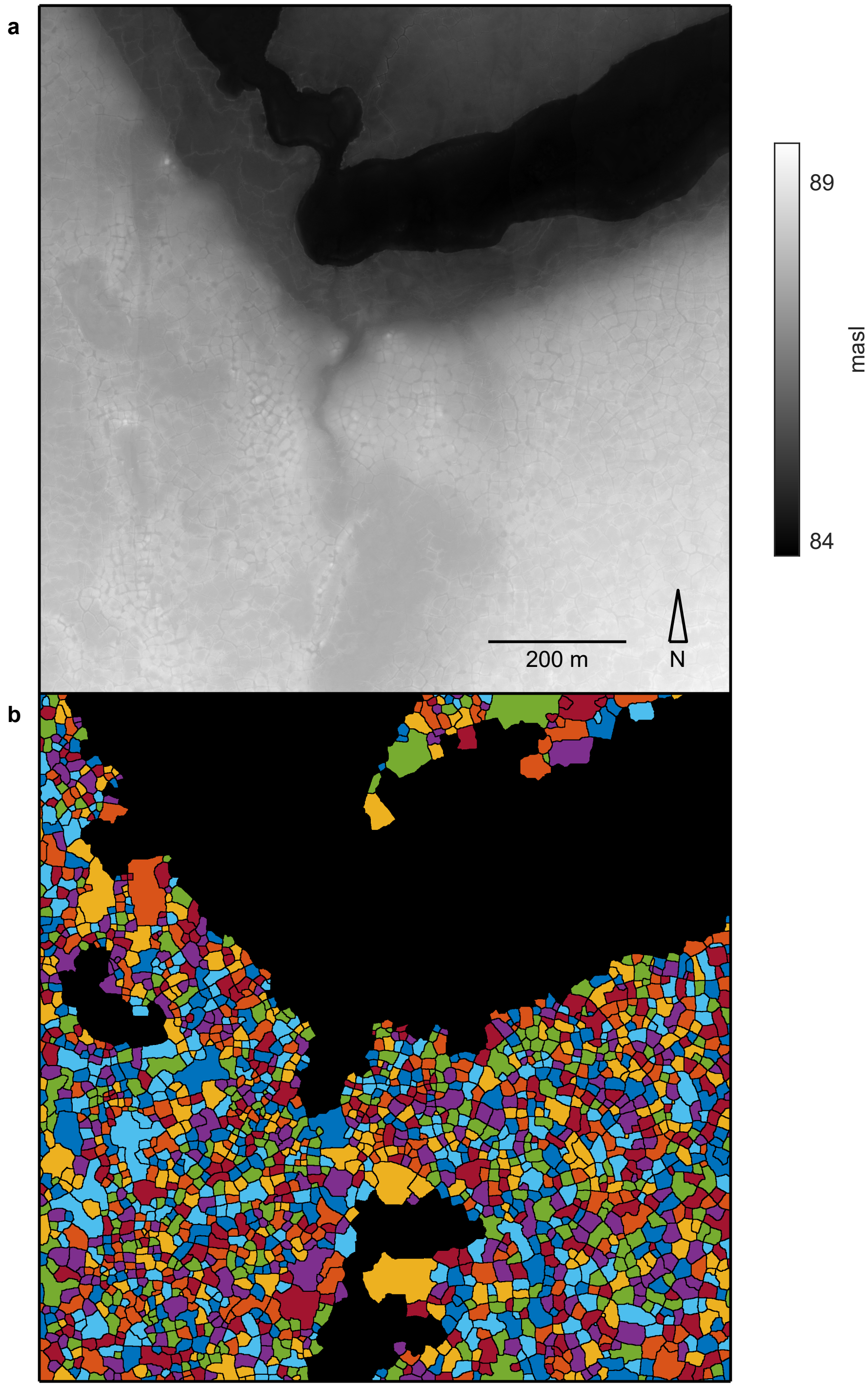

Figure S7. 50 cm DEM (**a**) and polygon delineation (**b**) at site Prudhoe-4.

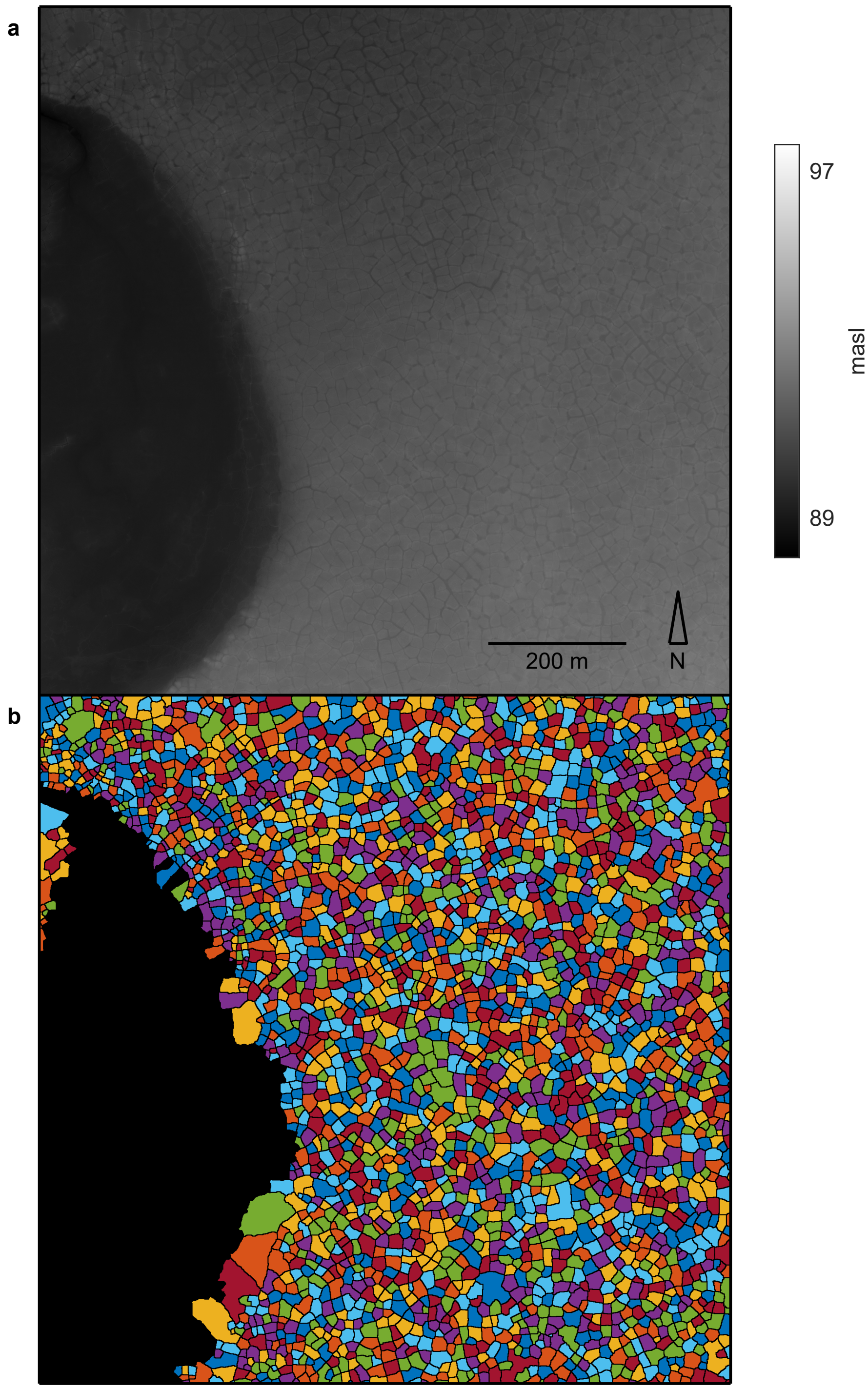

Figure S8. 50 cm DEM (**a**) and polygon delineation (**b**) at site Prudhoe-5.

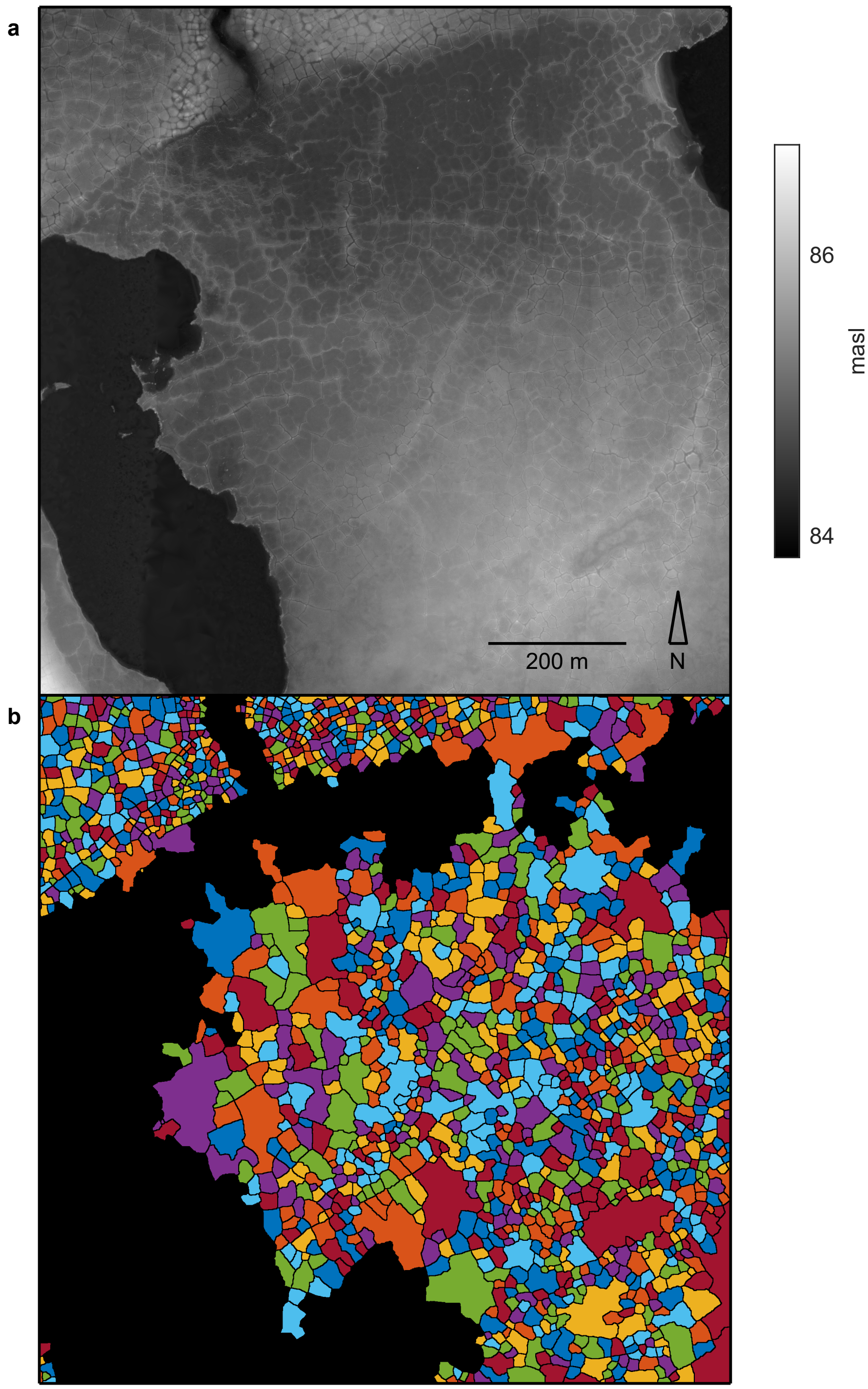

Figure S9. 50 cm DEM (**a**) and polygon delineation (**b**) at site Prudhoe-6.

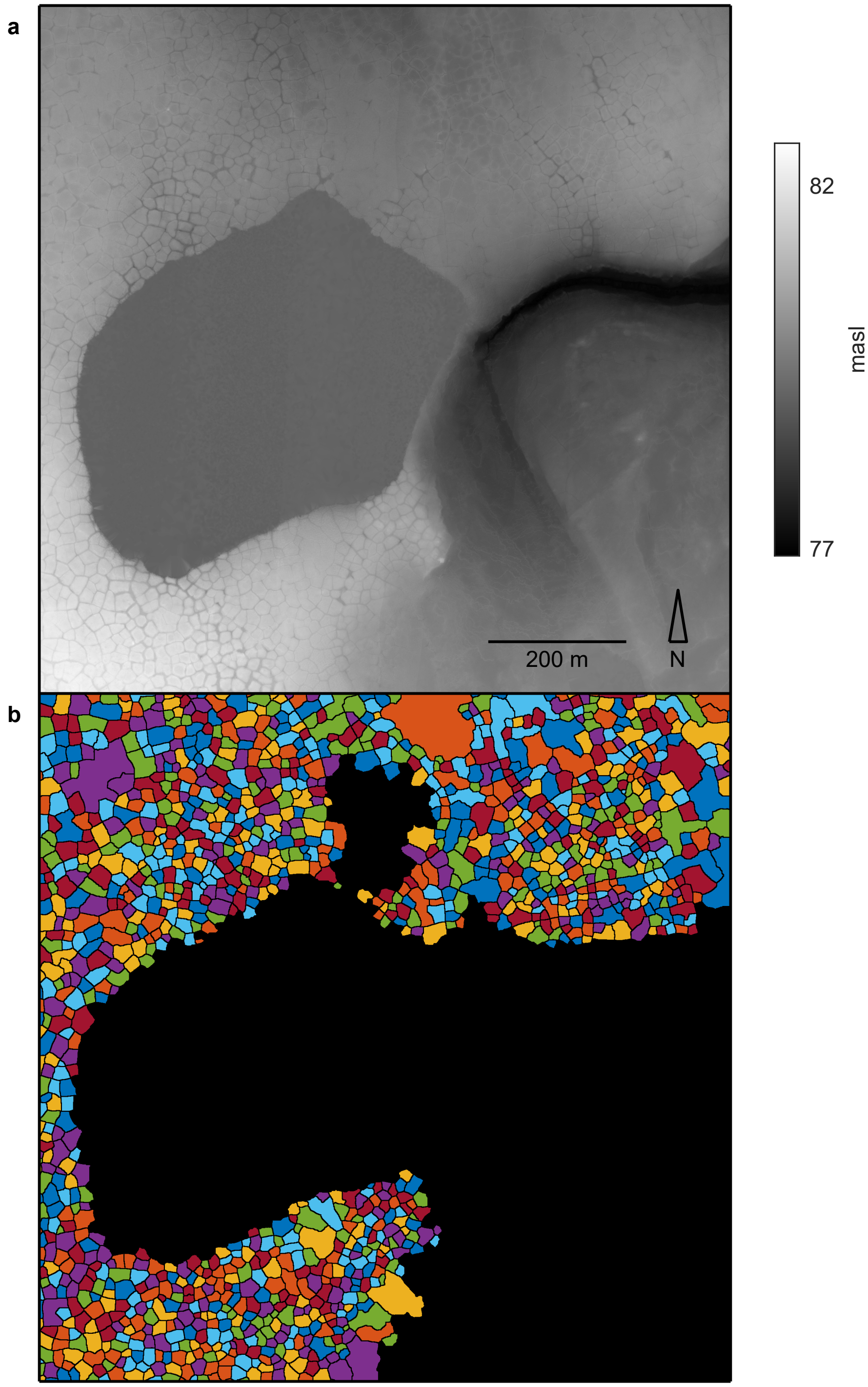

Figure S10. 50 cm DEM (**a**) and polygon delineation (**b**) at site Prudhoe-7.

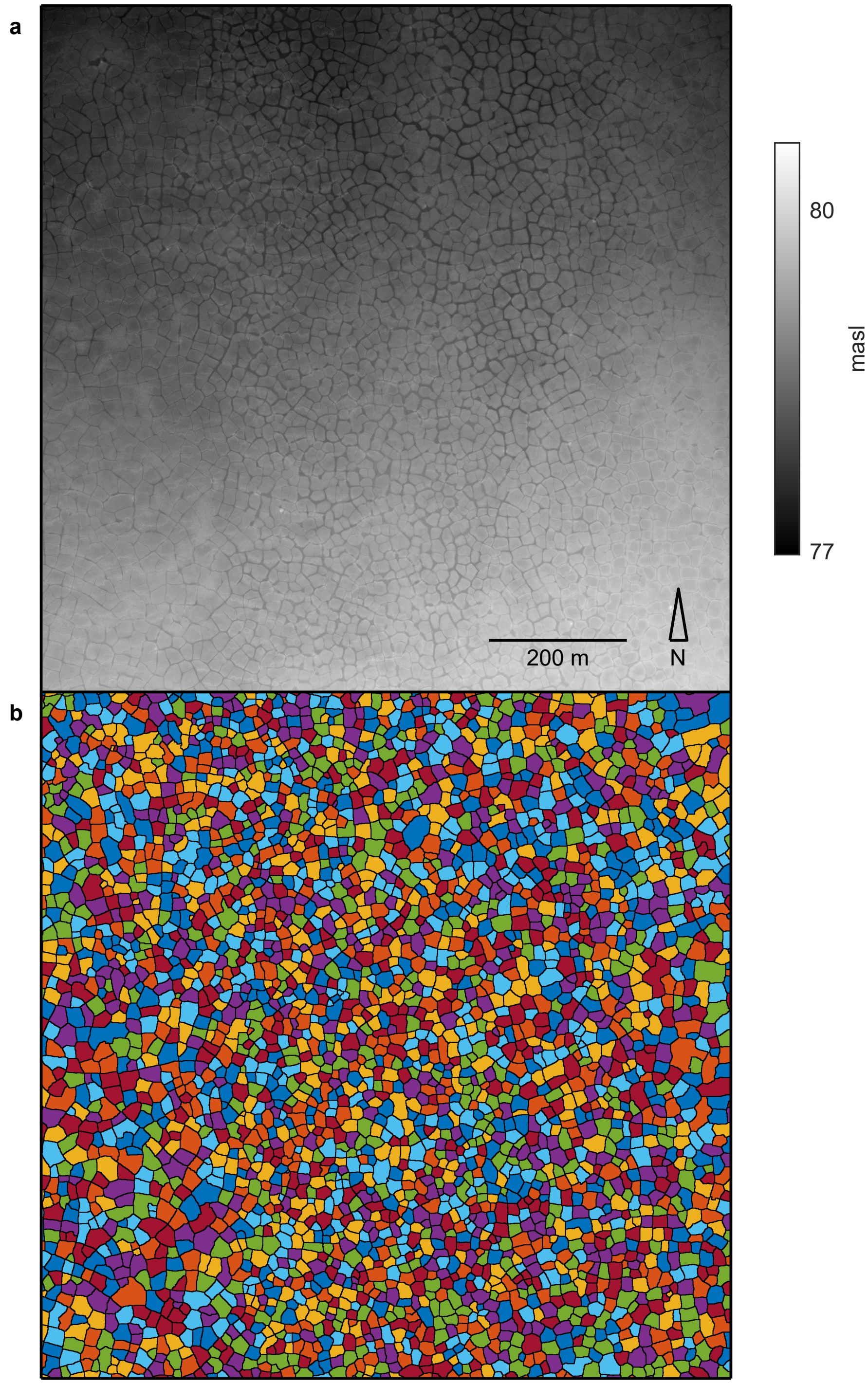

Figure S11. 50 cm DEM (**a**) and polygon delineation (**b**) at site Prudhoe-8.

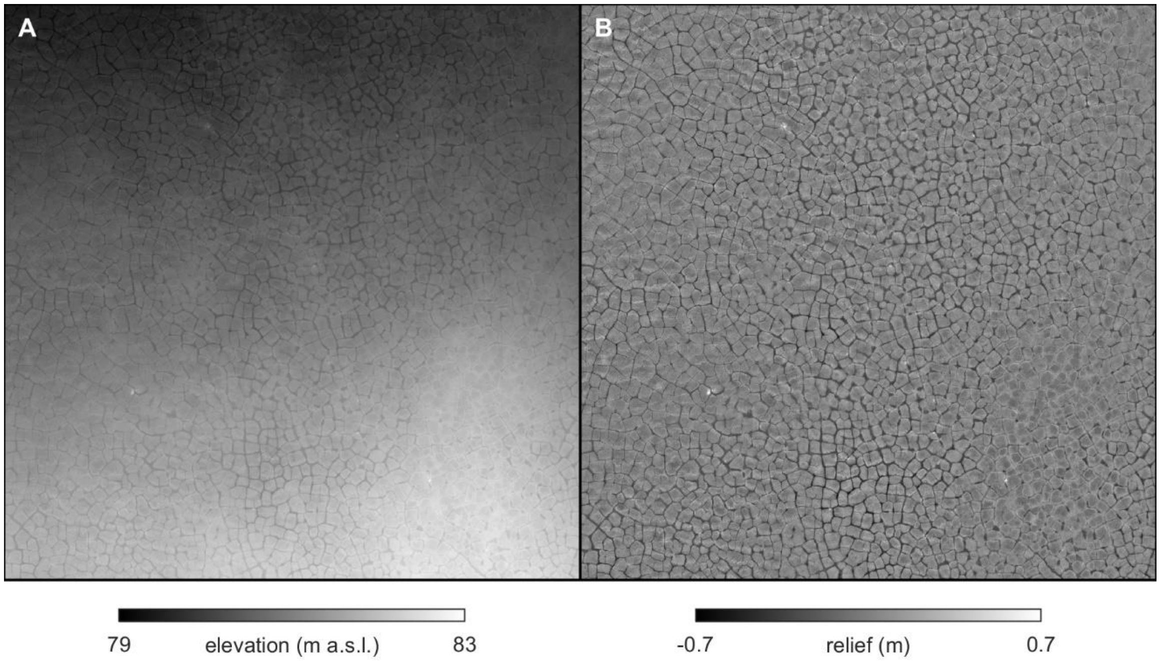

Figure S12. 50 cm DEM of the Prudhoe Bay training site before (**a**) and after (**b**) removing regional trends to isolate microtopography.

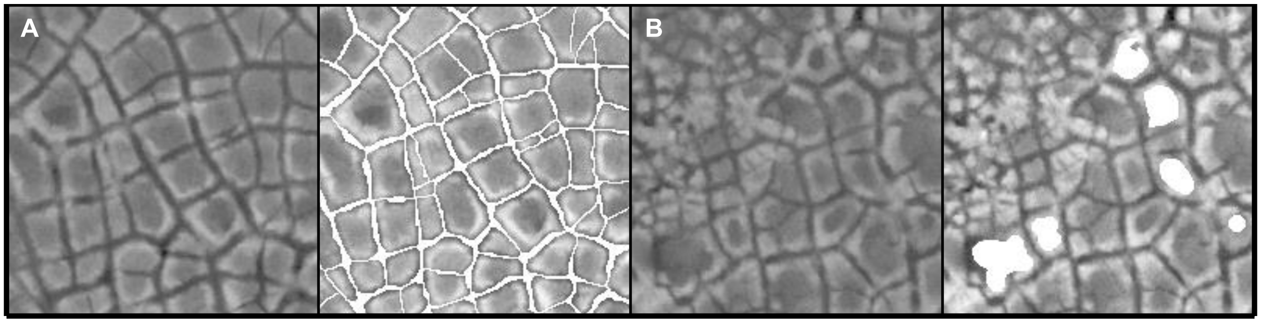

Figure S13. Samples of manually delineated data used to train the CNN, including a tile in which troughs are fully delineated (**a**) and a tile used to supplement the training deck with extra examples of non-trough pixels (**b**).

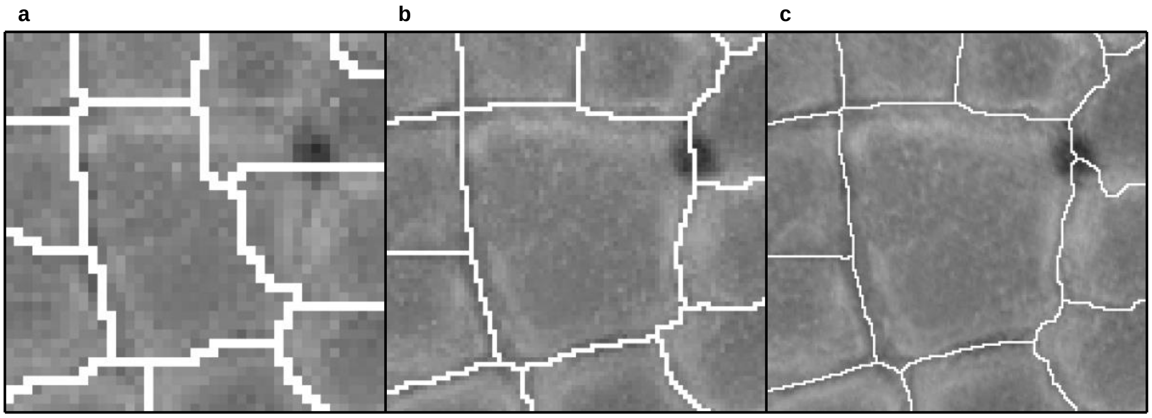

Figure S14. Results of the delineation algorithm on the same ice wedge polygon at 100 cm (**a**), 50 cm (**b**), and 25 cm (**c**) resolution. Each image is 40 m across. Note that anomalously low pixels in the polygon center in (**a**) are mistaken as polygon boundaries, incorrectly fragmenting the polygon.

Text S1. Comparison of training requirements and accuracy between CNN-watershed and Mask R-CNN algorithms.

Due to differences in the training and inference procedures used by each algorithm, training data requirements and accuracy are difficult to compare directly. Nonetheless, in several aspects, performance appears to be similar. In the present study, the CNN-watershed approach is trained initially on data derived from four manually-labeled 100 × 100 m tiles, representing 0.04 km^2. This training data is supplemented with extra examples of boundary and non-boundary features, the convex hulls of which sum to ~0.07 km^2, and the trained model is extrapolated across 10 km^2. The training to application ratio is therefore ~0.011, or 1.1%. In comparison, Mask R-CNN was trained on data from 340 90 × 90 m tiles, or ~2.75 km^2, then extrapolated across ~134 km^2, resulting in a training to application ratio of ~0.020 or 2.0% (Zhang et al., 2018). In general, within the area across which the CNN-watershed approach was applied, it was less likely than Mask R-CNN to fail to detect polygonal terrain, but more prone to mistakenly aggregate multiple ice wedge polygons into a single unit. These errors were particularly common at sites characterized by transitional terrain where ice wedge polygons grade into non-polygonal ground. It is reasonable to expect such mistakes in these areas, as microtopography is typically faint and polygons often appear to be bound incompletely by troughs. At one such site (Prudhoe-6), the number of incorrect conglomerate polygons by area delineated by the CNN-watershed algorithm was ~22% (Table 1). This number closely resembles the 21% of human-delineated polygons estimated to go undetected by Mask R-CNN in satellite-based optical imagery (Zhang et al., 2018).

Table S1. Architecture of our CNN.

Layer	Type	Neurons
1	Convolutional	8 arrays of 27×27
2	ReLU†	8 arrays of 27×27
3	Max-pooling	8 arrays of 9×9
4	ReLU	8 arrays of 9×9
5	Fully-connected	64
6	ReLU	64
7	Fully-connected	2
8	ReLU	2
9	Softmax	2

† - ReLu – rectified linear unit

Table S2. Results of manual validation at 100 cm and 25 cm resolution (sites are 1 km^2).

Site	Polygons identified	Polygonal area (%)	*% of polygons by instance* Whole	Fractional	Conglomerate	Non-polygonal	*% of polygons by area* Whole	Fractional	Conglomerate	Non-polygonal
Utqiagvik-1 (100 cm)	3058	74.3	73.4	18.6	6.2	1.8	65.5	16.6	13.4	4.1
Prudhoe-1 (100 cm)	3019	100	85.6	11.8	2.6	0.0	88.0	79.7	4.0	0.0
Utqiagvik-1 (25 cm)	2870	71.6	89.0	3.8	3.4	3.8	83.4	2.0	9.7	4.8
Prudhoe-1 (25 cm)	3193	100	93.6	3.4	2.4	0.6	94.0	1.6	4.3	0.1